Electronic growth of Pd(111) nanostructures on MoS_2

Timothy E. Kidd, Skylar Scott, Sophie Roberts, Ryan Carlile, Pavel V. Lukashev and Andrew J. Stollenwerk*

Physics Department University of Northern Iowa, Cedar Falls, Iowa 50614

ABSTRACT

Quantum confinement effects can induce the formation of discrete nanostructures with well-defined preferred heights in thin metallic films. In most systems such electronic growth modes are weak and limited to cryogenic conditions. Recently, however, we have discovered that metals grown upon van der Waals surfaces can exhibit electronic growth at, or even above, room temperature to spontaneously form well-defined and highly stable nanostructures. Here, we explore the initial stages of room temperature deposition of Pd onto MoS_2. We found that, even for minimal thicknesses, Pd spontaneously formed discrete islands with three atomic layers. The islands maintained this preferred height for nominal coverages below three atomic layers. At higher coverages, the preferred height switched abruptly to six atomic layers. Unlike previous studies using Au or Ag, the islands did not increase laterally with coverage, but rather increased in number with lateral size remaining about the same. The preferred heights in Pd/MoS_2 correlate to the Pd Fermi surface topography and are also consistent with thicknesses showing minima in the density of states at the Fermi level, which suggests that the electronic growth modes are the driving factors in these self-assembled Pd nanostructures. The Pd system shows a preference for

island nucleation compared to Au and Ag which grow laterally with increasing coverage. This is likely related to differences in bonding at the interface as Pd is typically much more reactive than Ag or Au.

KEYWORDS: self-assembly, quantum size effects, MoS_2, nanostructures, thin films, electronic growth

Tel:(319-273-7129) andrew.stollenwerk@uni.edu (Andrew J. Stollenwerk)

INTRODUCTION

Pd has a number of well-known applications for its catalytic properties in areas such as petroleum cracking, hydrogenation and other organic reactions [1]. Pd has also shown to be effective in the hydrogen energy sector for hydrogen storage and as a catalyst for hydrogen production. [2, 3]. Pd nanostructures are potentially more effective in these areas with potentially higher storage densities and catalytic rates tunable with physical size and density [4]. These factors make it desirable to determine methods for the controlled self-assembly of Pd nanostructures, which can be accomplished by understanding the growth mode of Pd on a given substrate. One substrate of interest is MoS_2, a semiconducting layered material belonging to the family of transition metal dichalcogenides (TMD). MoS_2 on its own is relatively inert, but also has various applications such as field-effect transistors (FETs) [5, 6], optoelectronic devices [7, 8], and notably hydrogen storage [9, 10]. With control over the growth of Pd on and in MoS_2, the Pd/MoS_2 system could find applications as a catalyst or in hydrogen storage.

Recently, it was shown that Au and Ag follow an electronic growth mode on MoS_2 [11, 12]. In these systems, the metals try to minimize their total energy by reducing the component associated with their electronic structure. On the nanometer scale, gaps can open at the Fermi level

(E_F) when the spatial dimensions correspond to the directional Fermi wavelength, which induces gaps at the Fermi energy and reduces the number of high energy electron states. In most systems, energy considerations due to the electronic structure are inconsequential as compared to surface kinetics, strain due to lattice mismatch, and surface free energy. Consequently, electronic growth modes are only observed in a small number of material systems and typically require cryogenic conditions for growth and stability [13-16]. The observation of this form of growth in Au and Ag on MoS_2 is believed to be the result of the weak interactions between the metal and the MoS_2 van der Waals surface. The interaction at the interface is sufficient to induce oriented growth in the <111> direction but the weak coupling allows high surface mobility to reach equilibrium conditions and minimizes issues related to strain. In fact, it is surprising to find epitaxial growth at all given the roughly 9% lattice mismatch of these metals with MoS_2 [17, 18].

Pd is a more reactive metal than either Ag or Au, but lattice mismatch between Pd and MoS_2 is only 0.5% [19]. Therefore, the Pd/MoS_2 system is promising for potential electronic growth research. Metal nanostructures exhibiting electronic growth modes spontaneously form discrete nanostructures with well-defined shapes and/or heights. Hence, this could provide a natural method for inducing self-assembled Pd nanostructures.

In this paper, we have used scanning tunneling microscopy (STM) to study the initial growth of Pd(111) on MoS_2. Our measurements indicate that Pd forms islands with preferred heights determined from local maxima in the height distribution relative to the MoS_2 substrate. These heights occurred at 0.61 ± 0.06 nm and 1.45 ± 0.09 nm, corresponding to three and six atomic layers, respectively. These preferred heights have a three atomic layer periodicity that strongly correlates with features in the Pd Fermi surface and also with Pd thicknesses that have minima in the calculated density of states (DOS) at the Fermi level (E_F). This correlation to the Pd electronic

structure suggests that the preferred heights seen in Pd/MoS_2 are indeed due to an electronic growth mode.

EXPERIMENTAL AND COMPUTATIONAL METHODS

Samples were prepared by depositing Pd onto the cleaved surface of commercially available MoS_2 (SPI supplies) in a vacuum chamber with a base pressure of 1×10^{-9} mbar. Deposition occurred at room temperature using a 2 mm Pd wire (99.95% pure) in a mini electron-beam evaporator (MANTIS QUAD-EV). A flux monitor was used to maintain a consistent deposition rate calculated to be approximately 0.1 Å/s from the resulting scanning tunneling microscopy images. Nominal thickness is defined as the thickness of the Pd film if it forms an atomically flat surface over an atomically flat substrate. Nominal thickness was determined from STM images and the error is estimated to be +/- 10% and used to calibrate the internal flux monitor. Coverages ranging from approximately 0.2 to 1.6 nm were prepared and transferred *in situ* to the adjacent STM head (Omicron). STM tips were electrochemically etched from a 0.25 mm W wire in a 5 M potassium hydroxide solution with a 5 V_{rms} bias. Scanning parameters used in this study were relatively consistent. The tunneling bias typically ranged from 0.75 to 1.5 V and the current set point varied from 0.5 to 5 nA. No significant differences were observed in the data between extremal scanning parameters.

We performed density functional calculations (DFT) of thin-film Pd in the (111) direction for film thicknesses from 0.46 to 3.00 nm. We used the projector augmented-wave method (PAW) [20], implemented in the Vienna *ab initio* simulation package (VASP) [21] within the generalized-gradient approximation (GGA) [22]. The integration method [23] was used with a 0.05 eV width of smearing along with a plane-wave cut-off energy of 500 eV and energy convergence criteria of 10^{-2} meV for atomic relaxation (resulting in the Hellmann-Feynman forces being less than 0.005

eV/Å), and 10^{-3} meV for the total energy and electronic structure calculations. A *k*-point mesh of 72 × 72 × 1 was used for the Brillouin-zone integration. Convergence of the results with respect to the *k*-mesh and cut-off energy was tested. A vacuum layer of 20 Å was imposed in all calculations to avoid the overlap of surface wave functions. Periodic boundary condition was imposed in all cases. For all calculations, the lattice geometry was fully optimized to obtain equilibrium structures. Some of the results and figures are obtained using the MedeA® software environment [24]. Most of the calculations are performed using Extreme Science and Engineering Discovery Environment (XSEDE) resources located at the Pittsburgh Supercomputing Center (PSC) [25], and the resources of the Center for Functional Nanomaterials (CFN) at Brookhaven National Laboratory (BNL).

RESULTS and DISCUSSION

Previous STM studies indicate Pd islands follow (111) growth on MoS_2 [26]. Although not as proliferant as in the images of Au and Ag on MoS_2 [11, 12, 27], some Pd islands form triangular shapes as seen in the images of Fig. 1 and expected from (111) growth. Cross sections of Pd islands reveal plateaued surfaces that were stable for at least several days at base pressure. The islands generally had a uniform distribution of heights (FWHM typically less than 1.0 nm) as exemplified by the height distributions depicted in Fig. 1. In these plots, the MoS_2 surface is marked by a dashed line and the location of the preferred height is labeled. The error of the preferred height is estimated to be equal to about 0.23 nm, a single monolayer of Pd(111) [28]. These results are typical across multiple depositions.

At the lower coverages found in Figs. 1a – 1c, Pd islands maintain a preferred height of about 0.6 nm as additional material is added to the surface. To accommodate the additional Pd without a change in height, the island density increases with little change in the lateral dimensions (within

the error associated with tip convolution). This is unlike the case of Ag or Au on MoS_2, in which metal atoms form nanostructures with larger lateral extents. [11, 12]. This may indicate that surface bonding effects play a larger role in the Pd/MoS_2 system, limiting the extent of epitaxial growth despite far superior lattice matching as compared to Ag and Au. As coverages exceed 0.6 nm, a new preferred height occurs at approximately 1.5 nm as seen in the height distributions in Figs. 1d – 1f. The island density also increases with coverage in this range with minimal change in the lateral dimensions. As the coverage approaches the preferred height, however, the islands do eventually coalesce into a relatively uniform film with pin hole defects extending down to the MoS_2 substrate as seen in Fig. 1f.

The data in Fig. 1 suggests that certain discrete heights of Pd islands are highly preferred over others. To further investigate this possibility, the preferred island heights are plotted as a function of nominal thickness in Fig. 2. The two plateaued regions seen in this plot corroborate the existence of energetically favorable island heights. The dashed lines on this plot indicate the average height of each plateau, excluding the four data points around the transitional point at approximately 0.6 nm. The first height of increased stability occurs at 0.61 nm ± 0.06 nm and the second occurs at 1.45 nm ± 0.09 nm, which corresponds to three and six Pd(111) atomic layers, respectively.

The samples were found to be highly stable with respect to time within the vacuum chamber, as our results remained consistent for at least several days. The relatively weak coupling between Pd and MoS_2 allowed the Pd islands to sometimes decouple from the MoS_2 surface during scanning. This phenomena, which has been seen in other metal-dichalcogenide interfaces [11], created significant challenges for systematic measurements. This could be one of the reasons there have been relatively few STM studies of the growth mechanism of Pd on MoS_2 and even fewer that explore the island heights at low coverage. One STM study indicates Pd islands grown at room

temperature have a consistent preferred height of approximately 0.85 nm at multiple low coverages [19], within one atomic layer of those in our study.

As discussed previously, the preferred heights seen here have many similarities to the electronic growth modes discovered in the growth of Au and Ag on MoS_2 [11, 12]. While Pd is more reactive, the much smaller lattice mismatch between Pd and MoS_2 would likely enhance the potential for epitaxial growth in this manner. Examination of the Fermi surface of Pd indicates a set of nesting vectors at approximately 0.65 nm [29]. Nesting vectors are a group of identical vectors that span parallel segments of the Fermi surface. If the dimensions of the structure match an integer value of a nesting vector, then a gap will form on the nested portions of the Fermi surface, reducing the overall electronic energy of the system.

This set of nesting vectors in Pd can be visualized in the 3D view of the portion of the Pd Fermi surface centered around Γ shown in Fig. 3a. It can be seen they span the inflection points of this portion along the surface normal direction, corresponding to the STM measurements showing an average preferred height interval of 0.7 +/- 0.1 nm. By symmetry, these nesting vectors span all the surface facets, representing a significant amount of the Fermi Surface DOS.

This gap opening at the Fermi energy would also be apparent in the DOS at the Fermi level. DFT calculations of free standing Pd(111) slabs also show periodic dips in the DOS at E_F at both three and six atomic layer thicknesses (Fig. 3b). This finding, in combination with correlation between Fermi nesting vectors and the preferred heights, indicate the Pd/MoS_2 system is highly influenced by electronic growth modes related to instabilities in the Pd electronic structure.

CONCLUSIONS

We have shown that Pd(111) islands grown on MoS_2 exhibit coverage dependent preferred heights. The periodic spacing of these heights is approximately three atomic layers, consistent with known nesting vectors on the Pd Fermi surface. These heights are energetically favorable due to the formation of gaps along the parallel faces associated with these nesting vectors, reducing the number of high energy electronic states. Further confirmation for an electronic growth mode is seen in DFT calculations of the DOS at the Fermi level of freestanding Pd(111) slabs. The quantization of island heights provides a measure of control over the dimensions of the Pd islands on MoS_2. Interestingly, at each preferred height there exists a large coverage in which both the island height and lateral size remains nearly constant. This enables a fine tuning of the island density and overall surface area of the Pd nanostructures which could be used to control or maximize catalytic properties.

Author Contributions

S. Scott, S. Roberts, and R. Carlile performed STM measurements, sample preparation, and DFT calculations. T. Kidd worked on analysis and drafting of the manuscript. P. Lukashev led DFT efforts and the associated theoretical analysis. A. Stollenwerk led efforts in STM measurements, Fermi surface analysis, and drafting of the manuscript.

Acknowledgements

The work was supported by Grant NO: DE-SC0020334 funded by the U.S. Department of Energy, Office of Science. T. Kidd was also supported by a PDA from the University of Northern Iowa. This work used the Extreme Science and Engineering Discovery Environment (XSEDE), which is supported by National Science Foundation grant number ACI-1548562. This work used the XSEDE Regular Memory (Bridges) and Storage (Bridges Pylon) at the Pittsburgh Supercomputing Center (PSC) through allocation TG-DMR180059, and the resources of the

Center for Functional Nanomaterials, which is a U.S. DOE Office of Science Facility, and the Scientific Data and Computing Center, a component of the Computational Science Initiative, at Brookhaven National Laboratory (BNL) under Contract No. DE-SC0012704.

Data Availability Statement

The data that supports the findings of this study are available within the article. Additional STM images supporting these findings may be made available upon reasonable request from the authors.

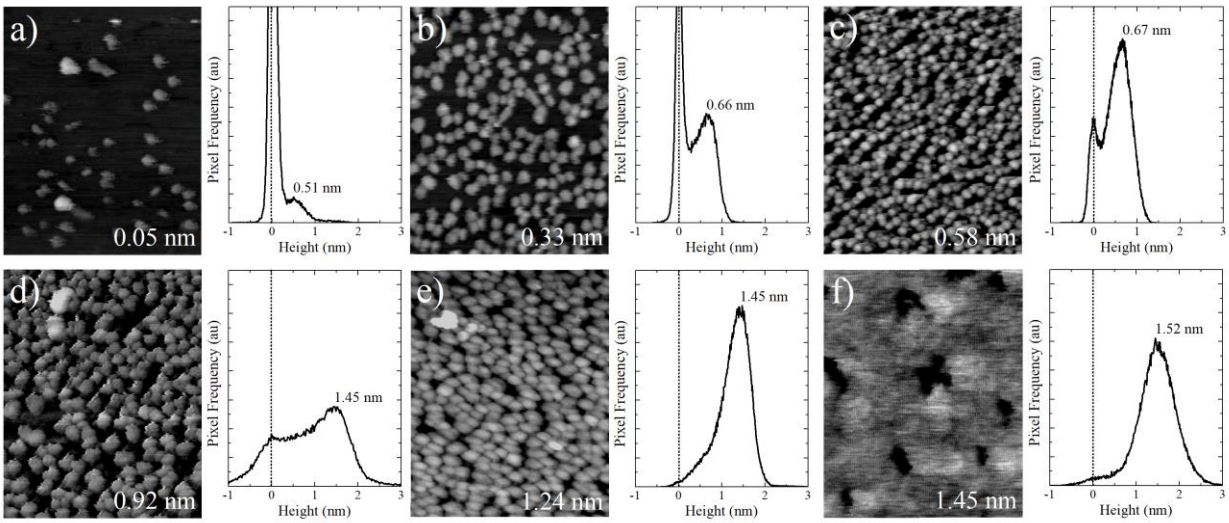

Figure 1: a) – f) Scanning tunneling microscopy images of Pd islands on MoS_2 at different nominal thicknesses indicated on each image. Corresponding height distributions are shown to the right of each image. The dashed line indicates the location of the MoS_2 substrate and the preferred island height is labeled on each plot. Each image is cropped to 40 nm × 50 nm.

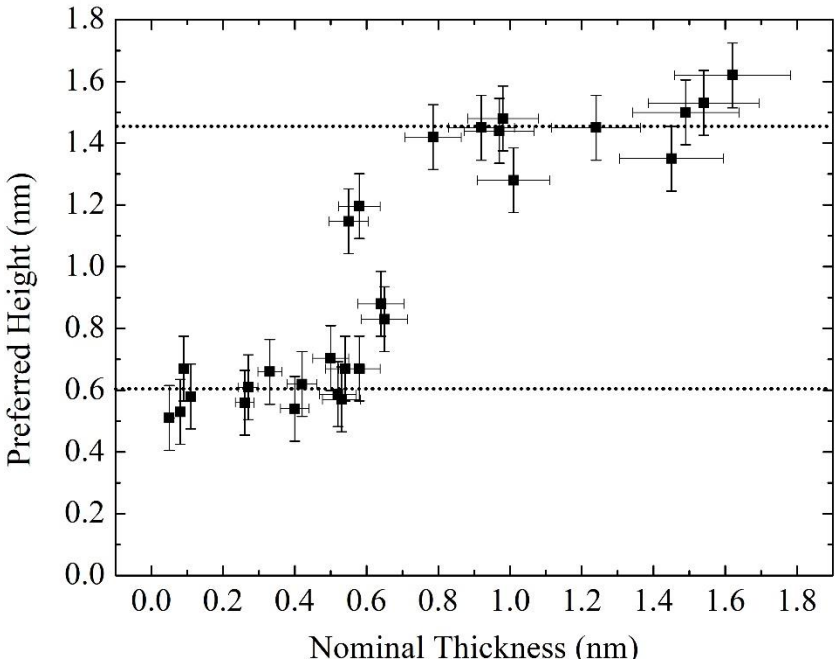

Figure 2: Preferred island heights as a function of nominal thickness. Two heights of increased stability are apparent. Horizontal, dashed lines indicate the average height of increased stability occurring at approximately 0.61 nm ± 0.06 nm and 1.45 nm ± 0.09 nm.

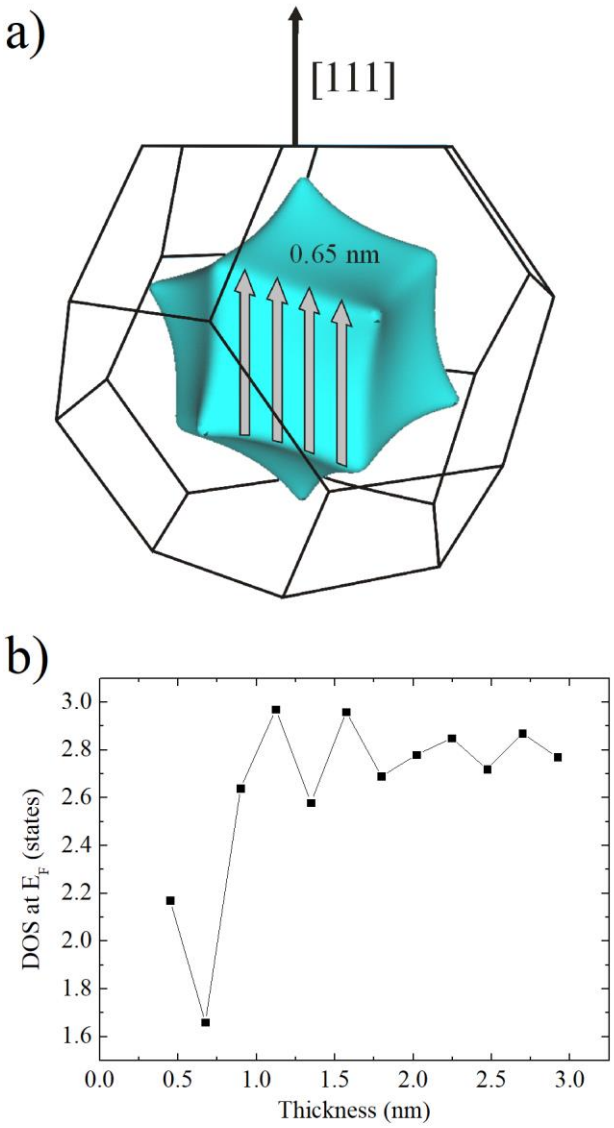

Figure 3: a) Portion of 3D Fermi surface of palladium (adapted from [30]). The grey arrows represent nesting vectors corresponding to a periodicity of 0.65 nm. b) Calculated DOS of freestanding Pd(111) slabs at the Fermi level as a function of Pd thickness. The first two minima occur at approximately 0.67 and 1.35 nm, respectively. These values agree well with the experimentally determined thicknesses of increased stability shown in Fig. 2.

[1] F. Wang, C. Li, L.-D. Sun, H. Wu, T. Ming, J. Wang, J.C. Yu, C.-H. Yan, Heteroepitaxial growth of high-index-faceted palladium nanoshells and their catalytic performance, Journal of the American Chemical Society, 133 (2011) 1106-1111.
[2] M. Navlani-García, K. Mori, D. Salinas-Torres, Y. Kuwahara, H. Yamashita, New Approaches Toward the Hydrogen Production From Formic Acid Dehydrogenation Over Pd-Based Heterogeneous Catalysts, Frontiers in Materials, 6 (2019).
[3] M. Yamauchi, R. Ikeda, H. Kitagawa, M. Takata, Nanosize Effects on Hydrogen Storage in Palladium, The Journal of Physical Chemistry C, 112 (2008) 3294-3299.
[4] S. Zhang, B. Jiang, K. Jiang, W.-B. Cai, Surfactant-Free Synthesis of Carbon-Supported Palladium Nanoparticles and Size-Dependent Hydrogen Production from Formic Acid–Formate Solution, ACS Applied Materials & Interfaces, 9 (2017) 24678-24687.
[5] B. Radisavljevic, A. Radenovic, J. Brivio, V. Giacometti, A. Kis, Single-layer MoS2 transistors, Nature Nanotechnology, 6 (2011) 147-150.
[6] S. Kim, A. Konar, W.-S. Hwang, J.H. Lee, J. Lee, J. Yang, C. Jung, H. Kim, J.-B. Yoo, J.-Y. Choi, Y.W. Jin, S.Y. Lee, D. Jena, W. Choi, K. Kim, High-mobility and low-power thin-film transistors based on multilayer MoS2 crystals, Nature Communications, 3 (2012) 1011.
[7] E. Singh, P. Singh, K.S. Kim, G.Y. Yeom, H.S. Nalwa, Flexible Molybdenum Disulfide (MoS2) Atomic Layers for Wearable Electronics and Optoelectronics, ACS Applied Materials & Interfaces, 11 (2019) 11061-11105.
[8] H. Wang, C. Li, P. Fang, Z. Zhang, J.Z. Zhang, Synthesis, properties, and optoelectronic applications of two-dimensional MoS2 and MoS2-based heterostructures, Chemical Society Reviews, 47 (2018) 6101-6127.
[9] J. Chen, J. Cao, J. Zhou, Y. Zhang, M. Li, W. Wang, J. Liu, X. Liu, Mechanism of highly enhanced hydrogen storage by two-dimensional 1T′ MoS2, Physical Chemistry Chemical Physics, 22 (2020) 430-436.
[10] J. Chen, N. Kuriyama, H. Yuan, H.T. Takeshita, T. Sakai, Electrochemical Hydrogen Storage in MoS2 Nanotubes, Journal of the American Chemical Society, 123 (2001) 11813-11814.
[11] T.E. Kidd, J. Weber, R. Holzapfel, K. Doore, A.J. Stollenwerk, Three-dimensional quantum size effects on the growth of Au islands on MoS2, Applied Physics Letters, 113 (2018) 191603.
[12] T.E. Kidd, E. O'Leary, A. Anderson, S. Scott, A.J. Stollenwerk, Self-assembled Ag(111) nanostructures induced by Fermi surface nesting, Physical Review B, 100 (2019) 235447.
[13] V. Yeh, L. Berbil-Bautista, C.Z. Wang, K.M. Ho, M.C. Tringides, Role of the Metal/Semiconductor Interface in Quantum Size Effects: Pb/Si(111), Physical Review Letters, 85 (2000) 5158-5161.
[14] W.B. Su, S.H. Chang, W.B. Jian, C.S. Chang, L.J. Chen, T.T. Tsong, Correlation between Quantized Electronic States and Oscillatory Thickness Relaxations of 2D Pb Islands on Si(111)-(7x7) Surfaces, Physical Review Letters, 86 (2001) 5116-5119.
[15] R. Otero, A.L. Vázquez de Parga, R. Miranda, Observation of preferred heights in Pb nanoislands: A quantum size effect, Physical Review B, 66 (2002) 115401.
[16] B.J. Hinch, C. Koziol, J.P. Toennies, G. Zhang, Evidence for Quantum Size Effects Observed by Helium Atom Scattering during the Growth of Pb on Cu(111), EPL (Europhysics Letters), 10 (1989) 341.
[17] S.G. Sørensen, H.G. Füchtbauer, A.K. Tuxen, A.S. Walton, J.V. Lauritsen, Structure and Electronic Properties of In Situ Synthesized Single-Layer MoS2 on a Gold Surface, ACS Nano, 8 (2014) 6788-6796.

[18] S.K. Mahatha, K.S.R. Menon, Quantum well states in Ag thin films on MoS2(0001) surfaces, Journal of Physics: Condensed Matter, 25 (2013) 115501.
[19] C. Gong, C. Huang, J. Miller, L. Cheng, Y. Hao, D. Cobden, J. Kim, R.S. Ruoff, R.M. Wallace, K. Cho, X. Xu, Y.J. Chabal, Metal Contacts on Physical Vapor Deposited Monolayer MoS2, ACS Nano, 7 (2013) 11350-11357.
[20] P.E. Blöchl, Projector augmented-wave method, Physical Review B, 50 (1994) 17953-17979.
[21] G. Kresse, D. Joubert, From ultrasoft pseudopotentials to the projector augmented-wave method, Physical Review B, 59 (1999) 1758-1775.
[22] J.P. Perdew, K. Burke, M. Ernzerhof, Generalized Gradient Approximation Made Simple, Physical Review Letters, 77 (1996) 3865-3868.
[23] M. Methfessel, A.T. Paxton, High-precision sampling for Brillouin-zone integration in metals, Physical Review B, 40 (1989) 3616-3621.
[24] MedeA-2.22, Materials Design, Inc., in, San Diego, CA, USA ,2017.
[25] J. Towns, T. Cockerill, M. Dahan, I. Foster, K.G. Gaither, Andrew, V. Hazlewood, S.L. Lathrop, Dave, G.D. Peterson, R. Roskies, J.R. Scott, N. Wilkens-Diehr, XSEDE: Accelerating scientific discovery, Computing in Science & Engineering, 16 (2014) 62.
[26] H. Dong, C. Gong, R. Addou, S. McDonnell, A. Azcatl, X. Qin, W. Wang, W. Wang, C.L. Hinkle, R.M. Wallace, Schottky Barrier Height of Pd/MoS2 Contact by Large Area Photoemission Spectroscopy, ACS Applied Materials & Interfaces, 9 (2017) 38977-38983.
[27] M. Cook, R. Palandech, K. Doore, Z. Ye, G. Ye, R. He, A.J. Stollenwerk, Influence of interface coupling on the electronic properties of the ${\text{Au/MoS}}_{2}$ junction, Physical Review B, 92 (2015) 201302.
[28] A. Venäläinen, K. Meinander, M. Räisänen, V. Tuboltsev, J. Räisänen, Metallization of self-assembled organic monolayer surfaces by Pd nanocluster deposition, Surface Science, 677 (2018) 68-77.
[29] M.D. Stiles, Exchange coupling in magnetic heterostructures, Physical Review B, 48 (1993) 7238-7258.
[30] T.-S. Choy, J. Naset, S. Hershfield, C. Stanton, J. Chen, A Database of Fermi Surfaces in Virtual Reality Modeling Language, APS, (2000) L36. 042.